HAL
open science

Dramatic impact of pressure and annealing temperature on the properties of sputtered ferroelectric HZO layers

Jordan Bouaziz, Pédro Rojo Romeo, Nicolas Baboux, Raluca Negrea, Lucian Pintilie, Bertrand Vilquin

To cite this version:

Jordan Bouaziz, Pédro Rojo Romeo, Nicolas Baboux, Raluca Negrea, Lucian Pintilie, et al.. Dramatic impact of pressure and annealing temperature on the properties of sputtered ferroelectric HZO layers. APL Materials, 2019, 7 (8), pp.081109. 10.1063/1.5110894 . hal-02273286

HAL Id: hal-02273286

https://hal.science/hal-02273286v1

Submitted on 28 Aug 2019

HAL is a multi-disciplinary open access archive for the deposit and dissemination of scientific research documents, whether they are published or not. The documents may come from teaching and research institutions in France or abroad, or from public or private research centers.

L'archive ouverte pluridisciplinaire **HAL**, est destinée au dépôt et à la diffusion de documents scientifiques de niveau recherche, publiés ou non, émanant des établissements d'enseignement et de recherche français ou étrangers, des laboratoires publics ou privés.

APL Materials

Dramatic impact of pressure and annealing temperature on the properties of sputtered ferroelectric HZO layers

Cite as: APL Mater. **7**, 081109 (2019); https://doi.org/10.1063/1.5110894
Submitted: 21 May 2019 . Accepted: 26 July 2019 . Published Online: 14 August 2019

Jordan Bouaziz, Pedro Rojo Romeo, Nicolas Baboux, Raluca Negrea, Lucian Pintilie, and Bertrand Vilquin

View Online Export Citation CrossMark

ARTICLES YOU MAY BE INTERESTED IN

Ferroelectricity in $YO_{1.5}$-HfO_2 films around 1μm in thickness
Applied Physics Letters **115**, 032901 (2019); https://doi.org/10.1063/1.5097880

Switching dynamics of ferroelectric HfO_2-ZrO_2 with various ZrO_2 contents
Applied Physics Letters **114**, 142902 (2019); https://doi.org/10.1063/1.5093793

Ultrafast measurements of polarization switching dynamics on ferroelectric and anti-ferroelectric hafnium zirconium oxide
Applied Physics Letters **115**, 072107 (2019); https://doi.org/10.1063/1.5098786

AMERICAN ELEMENTS
THE ADVANCED MATERIALS MANUFACTURER®
American Elements opens up a world of possibilities so you can **Now Invent!**
Over 15,000 certified high purity laboratory chemicals, metals, & advanced materials and a state-of-the-art Research Center. Printable GHS-compliant Safety Data Sheets. Thousands of new products. And much more. All on a secure multi-language "Mobile Responsive" platform.
Now Invent.™
The Next Generation of Material Science Catalogs
www.americanelements.com

© 2019 Author(s).

Dramatic impact of pressure and annealing temperature on the properties of sputtered ferroelectric HZO layers

Cite as: APL Mater. 7, 081109 (2019); doi: 10.1063/1.5110894
Submitted: 21 May 2019 • Accepted: 26 July 2019 •
Published Online: 14 August 2019

View Online Export Citation CrossMark

Jordan Bouaziz,[1,2,a)] Pedro Rojo Romeo,[1,b)] Nicolas Baboux,[2,c)] Raluca Negrea,[3,d)] Lucian Pintilie,[3,e)] and Bertrand Vilquin[1,f)]

AFFILIATIONS

[1] Université de Lyon, Institut des Nanotechnologies de Lyon (UMR5270/CNRS), Ecole Centrale de Lyon, 36 Avenue Guy de Collongue, F-69134 Ecully Cedex, France
[2] Université de Lyon, Institut des Nanotechnologies de Lyon (UMR5270/CNRS), INSA, Bât. Blaise Pascal, 7 Avenue Jean Capelle, F-69621 Villeurbanne Cedex, France
[3] National Institute of Materials Physics, Atomistilor 405A, Magurele, 077125, Romania

[a)] **Electronic mail:** jordan.bouaziz@insa-lyon.fr
[b)] **Electronic mail:** pedro.rojo-romeo@ec-lyon.fr
[c)] **Electronic mail:** nicolas.baboux@insa-lyon.fr
[d)] **Electronic mail:** raluca.damian@infim.ro
[e)] **Electronic mail:** pintilie@infim.ro
[f)] **Electronic mail:** bertrand.vilquin@ec-lyon.fr

ABSTRACT

The crystallization of ferroelectric (Hf,Zr)O_2 thin films is achieved by playing on the deposition pressure during reactive magnetron sputtering from a Hf/Zr metallic target. Postdeposition annealing was tried at different temperatures in order to optimize the quality of the samples. Structural characterizations are performed by transmission electron microscopy (TEM) and electrical characterizations are carried out. TEM analyses reveal that the samples deposited at a low working pressure show no orthorhombic phase, and thus are not ferroelectric, whereas the samples deposited at higher working pressure show the orthorhombic ferroelectric phase. The maximum remnant polarization is 6 μC/cm^2 and is obtained for the sample annealed at 600 °C. The maximum cycles to breakdown is higher than 2×10^{10} cycles and is reached for the sample annealed at 400 °C. These results are discussed in the matter of phase transition and oxygen vacancies redistribution.

© 2019 Author(s). All article content, except where otherwise noted, is licensed under a Creative Commons Attribution (CC BY) license (http://creativecommons.org/licenses/by/4.0/). https://doi.org/10.1063/1.5110894

I. INTRODUCTION

The discovery of ferroelectricity in Si-doped HfO_2 has been published in 2011 by Böscke *et al.*[1] Meanwhile, many publications have been written on the subject. In their 2018 review, Park *et al.*[2] presented a figure showing the impressively growing number of articles dealing with this subject. The reason for this success is due to the fact that ferroelectricity, in this family of materials, has the advantage to be theoretically optimized for a film thickness of 10 nm. It makes it suitable for a wide variety of applications such as ferroelectric random-access memories (FRAM), ferroelectric field-effect transistors (FeFETs), ferroelectric tunneling junctions (FTJ), steep-slope devices, and synaptic devices.

Many dopants have been used since 2011. Among them, Zr dopant is probably the most addressed since it allows the use of the lowest temperatures of all dopants, and both HfO_2 and ZrO_2 are used in Si CMOS[3] and/or DRAM mass production.[4]

However, most publications are focused on atomic layer deposition (ALD) as it has been previously mentioned by Bouaziz *et al.*[5] in order to deposit the (Hf, Zr)O_2 layer. Despite many advantages such as layer by layer growth and covering large areas,

© Author(s) 2019

the ALD rate is low compared to the physical vapor deposition (PVD) processes. Moreover, electrodes are often deposited by PVD because it could enhance ferroelectricity, at least if the top electrode is deposited by PVD.[6] Consequently, it could be interesting to have an operational process with a rapid deposition rate.

Indeed, we investigate the (Hf, Zr)O_2 layers capped between two TiN electrodes deposited by reactive magnetron sputtering. All depositions are performed at room temperature in the same sputtering chamber. The (Hf, Zr)O_2 solid solution is deposited from a Hf/Zr target with O_2 as the reactive gas. Chemical and structural characterizations are led by transmission electron microscopy (TEM). Electrical characterizations are carried out in order to compare with literature the change of the remnant polarization P_r as a function of the number of applied electrical field cycling. This change is characterized by the wake-up effect, the fatigue, and the breakdown.

II. EXPERIMENTAL DETAILS

A. Fabrication

Before deposition, the Si (100) oriented substrate is cleaned in acetone and ethanol, and then the native oxide layer is removed by buffered oxide etch (BOE) process. All depositions are carried out with a magnetron sputtering machine at room temperature: an AC-450 sputtering machine by Alliance Concept. TiN thin films are deposited by radio frequency (RF) magnetron reactive sputtering using a high purity Ti target in a mixture of argon and nitrogen gas. The bottom electrode (BE) is 100 nm-thick, and the top electrode (TE) is 50 nm-thick.

10 nm-thick (Hf, Zr)O_2 thin films were deposited onto the TiN BE using two different pressures, 5×10^{-2} mbar and 5×10^{-3} mbar, in order to obtain different microstructures. UV photolithography is used to obtain a top contact: 100 nm-thick Pt for electrical and mechanical contacts. Finally, the samples are annealed at three different temperatures in a rapid thermal annealing (RTA) furnace. Table I describes the fabrication settings for TiN and (Hf, Zr)O_2.

Characterizations are performed on annealed samples. Si/TiN/(Hf, Zr)O_2/TiN/Pt structures are called LP (for "Low Pressure") process when it refers to samples fabricated at 5×10^{-3} mbar and HP (for "High Pressure") process when it refers to samples fabricated at 5×10^{-2} mbar.

B. Characterization

The microstructural investigations of the specimens were performed by transmission analytical electron microscopy (TEM) using a JEM ARM 200F high resolution electron microscope operated at 200 kV. The samples were analyzed in the microscope in conventional (diffraction contrast imaging) and high resolution modes, with fixed and parallel beams (TEM/HRTEM). Cross-section TEM specimens have been prepared from the samples by mechanically polishing down to ca. 30 μm, followed by ion milling in a Gatan PIPS machine at 4 kV accelerating voltage and 7° incidence angle. Low-voltage (2 kV) milling was used as the final ion polishing stage in order to reduce the amorphous surface layer enveloping the specimen. Structural phases were identified using selected area electron diffraction (SAED) and filtered Fourier transformation (FFT).

All electrical measurements were performed on 20 μm diameter capacitors using a probe station and a setup consisting in an arbitrary waveform generator (Nippon Factory WF1966), a transimpedance current amplifier (Keithley 428), and a 12 bits digital storage oscilloscope (Nicolet Integra 40). The transimpedance

TABLE I. Film growth conditions.

Sputtering		
Target-substrate distance	8 cm	
Base pressure	$<5 \times 10^{-7}$ mbar	
Ignition pressure	5×10^{-2} mbar	
Deposited elements	TiN	(Hf, Zr)O_2
Substrate	Si(100)	Si(100)/TiN
Target	Ti (99.995%)	Hf/Zr (99.9%)
Target RF power	300 W	100 W
Holder DC bias voltage	60 V	None
Gas	Ar = 50 sccm; N_2 = 3 sccm	Ar = 50 sccm; O_2 = 10 sccm
Working pressure	5×10^{-3} mbar	5×10^{-2} mbar or 5×10^{-3} mbar
Deposition speed	5.0 nm/min	≈0.83 nm/min for 5×10^{-2} mbar ≈1.0 nm/min for 5×10^{-3} mbar
Rapid thermal annealing (RTA) conditions		
Temperature variation	400/500/600 °C	
Atmosphere	N_2	
Time	30 s	

© Author(s) 2019

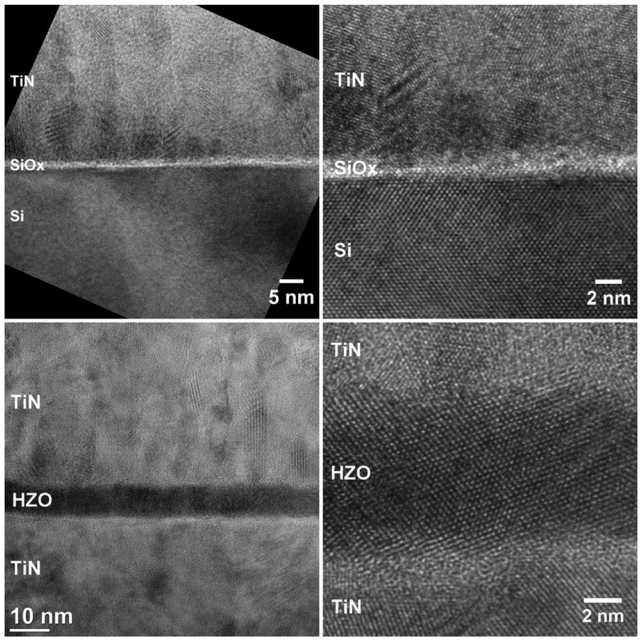

FIG. 1. HRTEM images showing the interfaces between the TiN and Si substrate and between the TiN layers and (Hf, Zr)O_2 thin film on a LP sample annealed at 500 °C.

amplifier is used to create a virtual ground with a feedback resistor to measure the current. After acquisition, the charge is obtained by numerical integration and normalization.

P-E curves were obtained using the 5 pulses PUND train: a negative setting pulse followed by two positive ones (P and U) and finally two negative ones (N and D). PUND pulses had a triangular shape, with an amplitude of 3.5 V and a rising/falling time of 100 μs [which corresponds to a frequency of 2500 Hz = 1/(4 × 100 μs) as reported on commercial testers].

To test their endurance, the capacitors were cycled, usually until breakdown. To eventually evidence an initial rapid change of properties, tests were started with 10 PUND loops (cycles 1–10). Then, bipolar square pulses of 3.5 V amplitude were applied with the frequency set either to 2.5 kHz or to 1 MHz.

III. RESULTS AND DISCUSSIONS

A. TEM Structural Characterization

The samples have been analyzed by TEM with low magnification, HRTEM and SAED. Six samples have been analyzed by TEM, three for each LP and HP processes. These three samples were annealed by RTA at 400 °C, 500 °C, and 600 °C. Results are shown in Figs. 1–3.

Figure 1 shows the HRTEM images of the LP sample annealed at 500 °C. Two interfacial layers (IL) can be seen. The first interfacial layer is located between the TiN BE and the Si substrate. Therefore, we consider this layer to be SiO_x. The other IL is located between TiN BE and (Hf,Zr)O_2. We assume this layer should be TiO_xN_y according to the process described by Esaka *et al.*[7] This interfacial layer could also play an important role since the distribution of oxygen vacancies in ferroelectric (Hf,Zr)O_2 is critical during the cycling process.[8–10] Although Fig. 1 shows the results for the LP sample annealed at 500 °C, the same ILs have been observed on every sample.

Figure 2 shows the results for LP process at different temperatures. TEM images confirm the thicknesses of the BE and TE. The (Hf, Zr)O_2 layers are actually 12 nm thick. No orthorhombic phase (o-phase), which characterized ferroelectricity in this material, can be seen. Only the monoclinic phase (m-phase) is observed. Consequently, at 5 × 10^{-3} mbar, it seems impossible with our equipment to grow the o-phase.

Figure 3 shows the results for the HP samples. The thicknesses of the TiN BE is found to be around 110 nm for the three samples

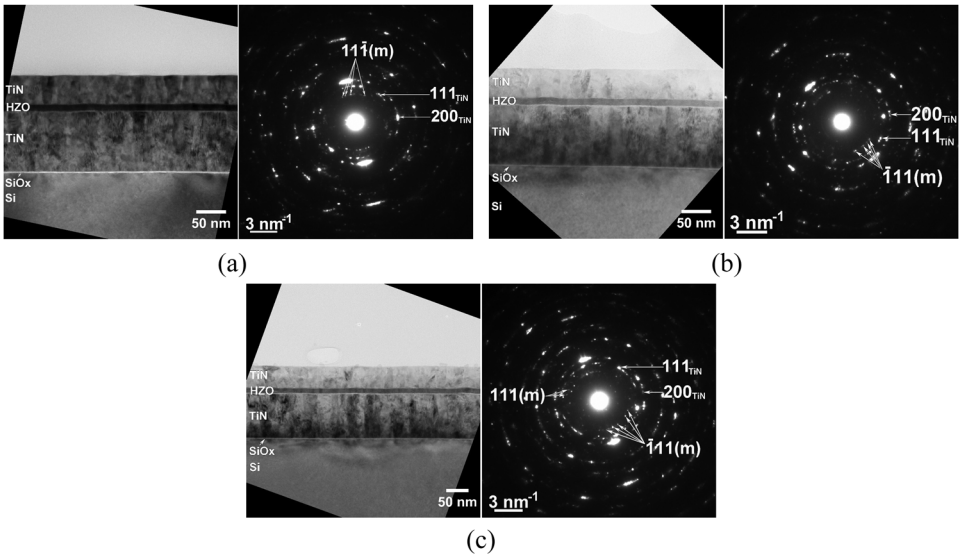

FIG. 2. HRTEM images showing LP TiN/(Hf, Zr)O_2/TiN layers and the corresponding diffraction patterns for the samples annealed at (a) 400 °C, (b) 500 °C, and (c) 600 °C.

© Author(s) 2019

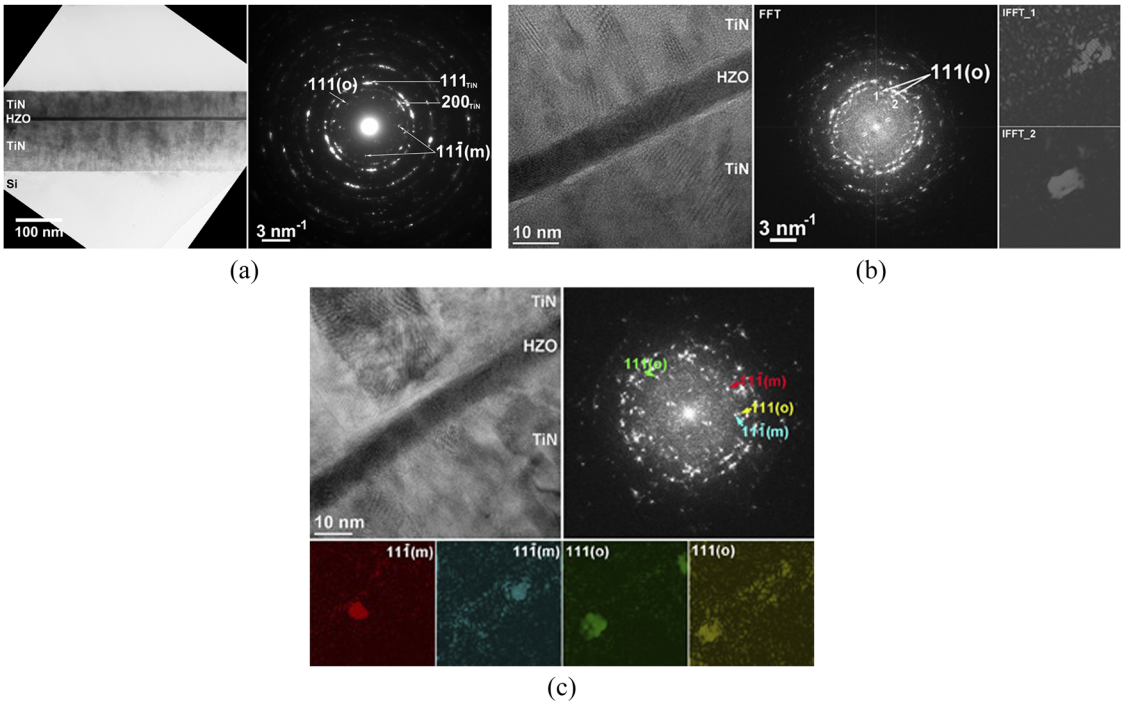

FIG. 3. TEM, HRTEM, and SAED images showing HP TiN/(Hf, Zr)O_2/TiN layers and the corresponding FFT patterns for samples annealed at (a) 400 °C, (b) 500 °C, and (c) 600 °C.

and is around 60 nm for the TE—except for the sample annealed at 600 °C, where the thickness was found to be 72 nm. The thickness of the (Hf, Zr)O_2 layers is between 9 nm and 10 nm for each sample. In Fig. 3(a), we can notice a complex SAED pattern corresponding to the sample annealed at 400 °C. In this pattern, the main rings, the most intense and well defined, belong to the TiN layer and these rings can also be observed in the FFT pattern in Figs. 3(b) and 3(c) corresponding to the samples annealed at 500 °C and 600 °C. These rings were not pointed out in order to simplify the figures. The HZO spots are very fine and less intense due to the layer thickness and grain width. The monoclinic and orthorhombic phases of HZO were indicated in SAED and FFT patterns as a result of the measurements; the distance between the shown spot and the central spot was measured and the corresponding interplanar distance calculated. In order to determine the correct phase and space group of the material, the obtained result is compared with the database. The main difference between the monoclinic and orthorhombic phase is made by the m(11-1) (with d = 3.14 Å) and o(111) (with d = 2.96 Å) lines. The difference between these lines (0.18 Å) can be easily evidenced in SAED and FFT patterns and confusion between these phases cannot be made. The presence of the o-phase is confirmed for each HP sample. The presence of the monoclinic phase is also confirmed on the 400 °C and 600 °C samples. No monoclinic phase has been seen on the sample annealed at 500 °C. However, in our previous work,[5] samples were fabricated with the exact same process. XRD measurements actually showed monoclinic peaks for HP samples annealed at 500 °C and 600 °C. Therefore, it is believed that the monoclinic phase is still present on the HP sample annealed at 500 °C, even if not shown in the HRTEM images [Fig. 3(b)]. Indeed, HRTEM measurements is very local unlike the XRD measurement which gives information on a large sample area (5 mm × 5 mm).

To conclude on TEM characterizations, the presence or absence of the o-phase in the thin (Hf, Zr)O_2 films seems to be highly related to working pressures. The different working pressures are assumed to cause a difference in the energy of the incident atoms during deposition. This energy is supposed to be lower in the case of a deposition at 5×10^{-2} mbar which could make the sample closer to the amorphous phase observed in ALD just after deposition and could explain why the sample shows o-phase after RTA.

B. Electrical Characterizations

Electrical characterizations were performed on the HP samples. Figure 4 presents the polarization P vs the electrical field E for the sample annealed at 600 °C after different number of cycles according to the sequence described in the experimental section. The classical wake-up effect[11] is observed. The remnant polarization P_r reaches 6 μC/cm^2 after 10^6 cycles and just before the breakdown happens. As it has been previously discussed, the low value of P_r is assumed to be due to stoichiometry issues.[5] However, one can note that P_r value has increased compared to our previous work. It is due to the change in the stress sequence that will be discussed in the next paragraphs.

The coercive electrical field E_c starts at 2.7 MV/cm^2 and reaches 1.2–1.3 MV/cm^2 after 10^6 cycles. The change of E_c values with

© Author(s) 2019

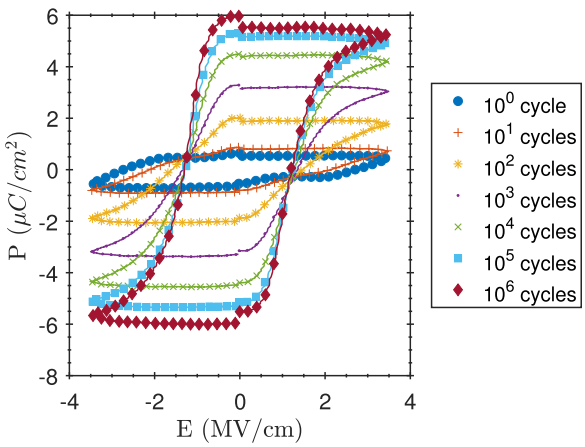

FIG. 4. P-E curve for the HP sample deposited and annealed at 600 °C for different number of cycles.

the number of cycles is symmetrical on almost every electrode. However, some articles show an increase of E_c from pristine to wake-up.[11] E_c change seems to be not clearly identified in literature. For instance, in the article written by Park *et al.* in 2016,[12] the change of E_c seems to increase at the beginning and then is decreasing. As a consequence, the change in E_c is not clearly understood.

Figure 5 compares the behaviors of the sum of the absolute values of the remnant positive polarization P_{r+} and the remnant negative polarization P_{r-} vs the number of cycles for the three samples. Note that after 10 cycles, there is a break in the slope of $|P_{r+}| + |P_{r-}|$ vs the number of cycles because only the PUND sequence was used during the first ten cycles. Then, the sequence with bipolar square pulses is used to stress the sample with the same amplitude and PUND sequence is used to measure. All symbols of the curve

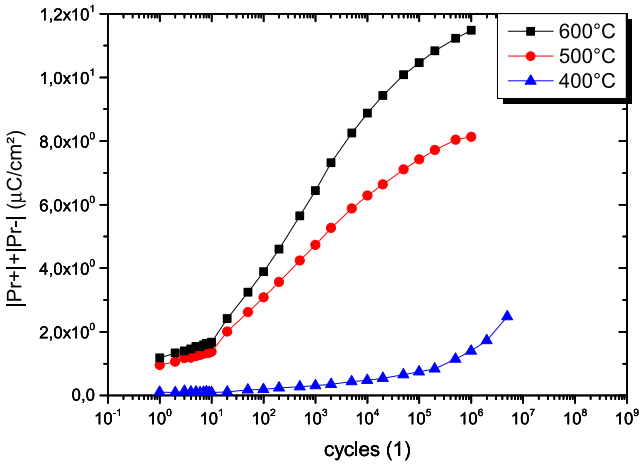

FIG. 5. Change of the remnant positive and negative polarization sum vs the number of cycles for HP samples annealed at three different temperatures. Stressing is carried out at 2.5 kHz with bipolar square pulses.

are extracted from the PUND sequence. Consequently, the fact that the stress sequence is used only after the first ten cycles explains the break in the slope.

P_r values increase more rapidly with RTA temperatures. It seems consistent with what has been previously observed.[13,14]

In ferroelectric HfO_2-based materials, 3 different stages corresponding to different states of the material can be distinguished by increasing the number of cycles: pristine, woken-up, and fatigued.[2] It corresponds to a first stage where there is an increase of P_r, a short stable stage where P_r is nearly constant and a decrease of P_r as a function of the number of cycles. This change is attributed to phase change[9,15,16] and oxygen vacancies displacements.[17–19]

Here, the samples have systematically reached the breakdown before the P_r decreasing except in one case [cf. Fig. 7(b)]. The fatigued stage is consequently nearly never observed.

The samples annealed at 500 °C and 600 °C have reached the stable stage before breaking down.

In our previous work,[5] the fact that an identical sample as the one annealed at 400 °C was not ferroelectric was mentioned. However, the stress sequence was performed with the same triangle as the one in PUND. It has been actually shown that the period (frequency) of the stress sequence strongly influences P_r and the number of cycles to breakdown.[11,19,20] Bipolar square pulses are more stressful than the triangle ones. Indeed, at a given period and frequency, the time at maximum voltage is much longer with squares than it is with triangles. Moreover, cycling beyond 10^6–10^7 cycles becomes unreasonably time consuming to be carried out with this former sequence. For both reasons, the transition from nonferroelectric to ferroelectric state was never reached with this former sequence.

Consequently, in our previous work,[5] it was thought that the sample annealed at 400 °C was not ferroelectric. In fact, Fig. 6(a) shows what was observed in these conditions. This behavior is typical of a dielectric and nonferroelectric capacitor and was previously observed until 10^6 cycles.

Using our new sequence of stress (with bipolar square pulses), it was possible to make the observation [Figs. 6(b) and 6(c)], respectively, after 10^5 cycles and just before the breakdown. As one can see, the sample, which was not ferroelectric during the first cycles, begins to present a switching current after $\approx 10^5$ cycles. This switching current is typical of ferroelectricity.

To go a step further, electrical characterizations were carried out with bipolar square pulses using a higher frequency (1 MHz). Indeed, previous works[11,19,20] predict the fact that the breakdown will happen at a higher number of cycles with a lower P_r.

Figure 7(a) is a zoomed in detailed view of Fig. 5 for the sample annealed at 400 °C, where the results are shown for 3 different electrodes. Figure 7(b) shows the result for a period of 1 μs. It corresponds to 1 MHz, which is the conventional frequency in microelectronics. It can be observed that the breakdown is reached between 1×10^{10} and 5×10^{10} cycles using three different electrodes at different locations on the sample. 10^{10} cycles is more than what is required for industrial applications. The same process has been tested at 500 °C and 600 °C. The same tendency is observed: the breakdown has appeared at higher cycling step, but they have reached only 10^7–10^8 cycles before breaking down. Moreover, P_r is decreasing when using higher frequency.

© Author(s) 2019

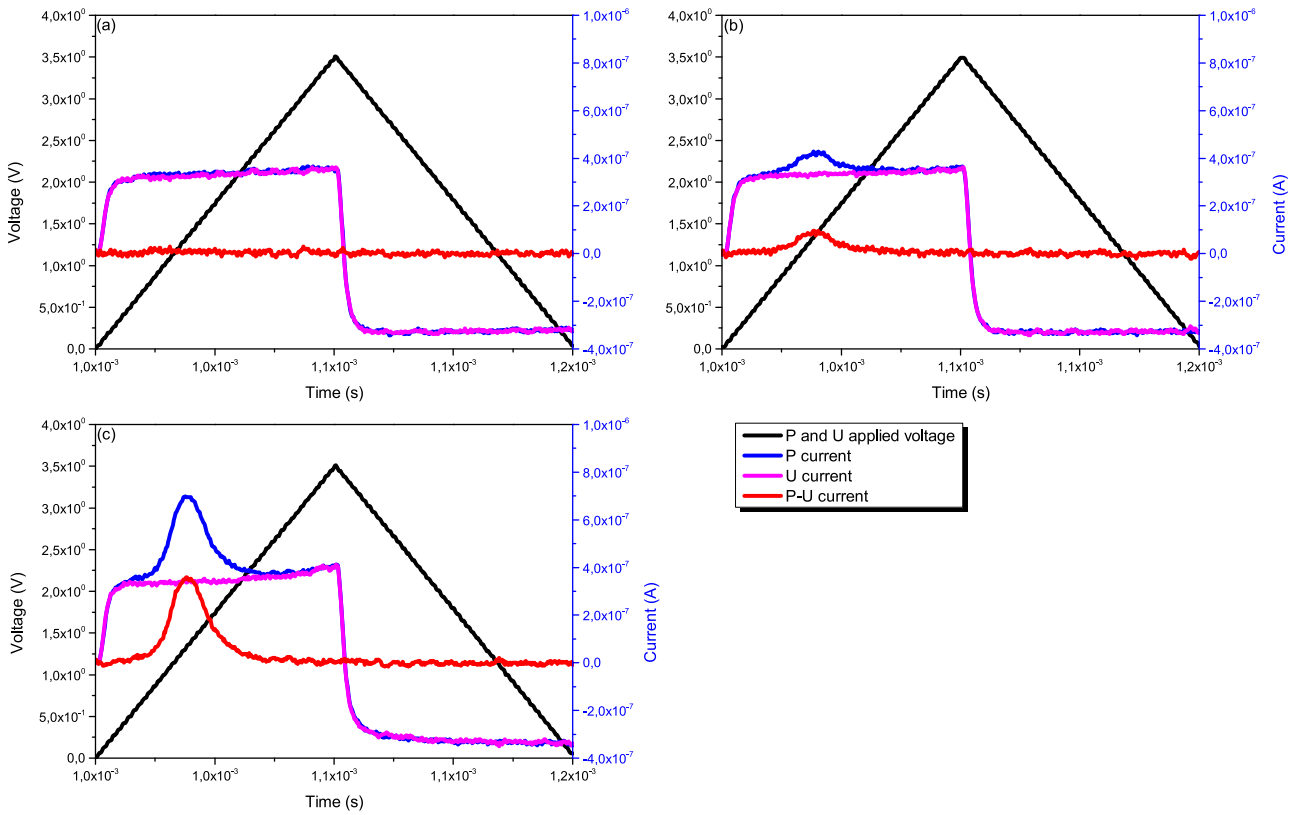

FIG. 6. P,U and P-U signal currents vs time of the HP sample annealed at 400 °C for (a) 1 cycle, (b) 10^5 cycles, and (c) just before breakdown.

A similar behavior was reported by Walters *et al.*[21] for a 5 nm HZO film grown by ALD and annealed at 500 °C. The film initially showed no polarization. However, electric field cycling was able to induce a polarization. This behavior could give several clues on the behavior of ferroelectric HfO_2-based materials. For instance, as-deposited ferroelectric HfO_2-based materials are supposed to be nonferroelectric and need an annealing step. The sample annealed at 400 °C does not show ferroelectriclike

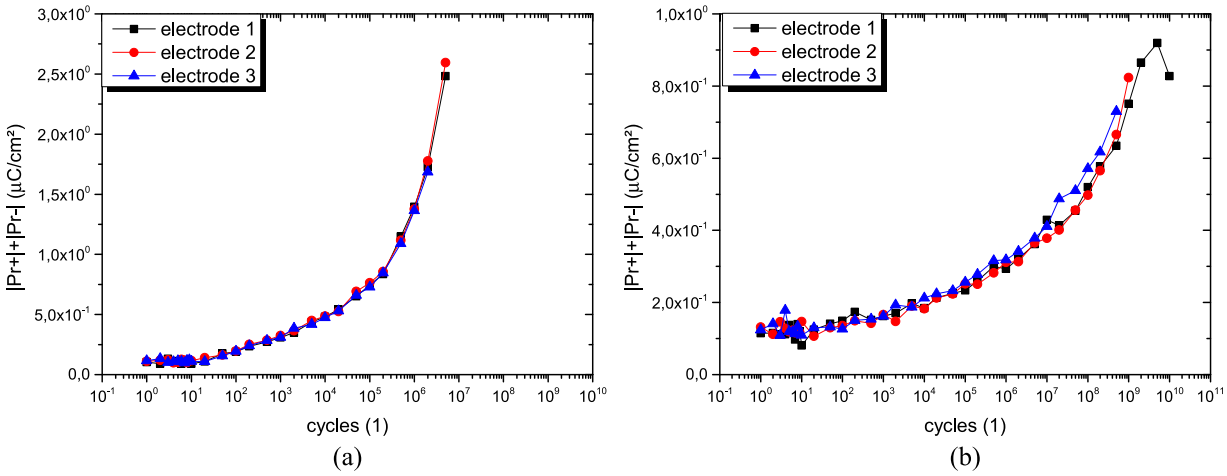

FIG. 7. Change of $|P_{r+}| + |P_{r-}|$ vs the number of cycles for the HP sample annealed at 400 °C tested on three different electrodes and using a period of (a) 400 μs (2.5 kHz) and (b) 1 μs (1 MHz).

© Author(s) 2019

behavior until 10^5–10^6 cycles depending on the frequency used. It could help in the understanding of the formation of the o-phase—which is generally admitted to correspond to the ferroelectric phase—during the annealing step. It could also help in the understanding of the wake-up, fatigue, and endurance mechanisms since they are assumed to be all related to phase transition[9,15,16] and oxygen vacancies redistribution.[17–19] These 3 phenomena are probably the biggest current issues preventing industrial applications to appear in the market.

IV. CONCLUSION

The structural characterization of (Hf,Zr)O_2 solid solutions have been performed by TEM. TEM measurements show the presence of IL not only between Si and TiN but also between TiN bottom electrode and (Hf, Zr)O_2. This last IL could play a role in the redistribution of oxygen vacancies during the pristine, woken-up, and fatigued state of the sample. The LP samples neither show o-phase nor ferroelectricity, whereas the HP samples show both properties. Electrical characterization revealed that the biggest P_r is reached for the sample annealed at 600 °C and is around 6 μC/cm^2. The sample annealed at 400 °C shows a surprising and an interesting behavior since it is not ferroelectric at the beginning of the cycle sequence, and it is needed to stress the sample to reach ferroelectric properties. Stressing the sample with lower frequency increases P_r, but the breakdown appears sooner. Hence, using bipolar square pulses with a shorter period of 1 μs (1 MHz) as stress, it has been possible to trigger ferroelectricity for the sample annealed at 400 °C and to reach a maximum of 5×10^{10} cycles before breakdown. This behavior is of crucial significance for further investigations dealing with phase change and oxygen vacancies redistribution in HfO_2-based materials. Their understanding is indeed the last challenge to overcome.

ACKNOWLEDGMENTS

This work was realized on the NanoLyon technology platform and has received funding from the European Union's Horizon 2020 research and innovation programme under Grant Agreement No. 780302. We thank GDR OxyFun for its financial support.

REFERENCES

[1] T. S. Böscke, J. Müller, D. Bräuhaus, U. Schröder, and U. Böttger, "Ferroelectricity in hafnium oxide thin films," Appl. Phys. Lett. **99**, 102903 (2011).

[2] M. H. Park, Y. H. Lee, T. Mikolajick, U. Schroeder, and C. S. Hwang, "Review and perspective on ferroelectric HfO_2-based thin films for memory applications," MRS Commun. **8**, 795 (2018).

[3] K. Kim, "From the future Si technology perspective: Challenges and opportunities," in *2010 International Electron Devices Meeting* (IEEE, 2010), pp. 1.1.1–1.1.9.

[4] D. James, "Recent innovations in DRAM manufacturing," in *2010 IEEE/SEMI Advanced Semiconductor Manufacturing Conference (ASMC)* (IEEE, 2010), pp. 264–269.

[5] J. Bouaziz, P. Rojo Romeo, N. Baboux, and B. Vilquin, "Characterization of ferroelectric hafnium/zirconium oxide solid solutions deposited by reactive magnetron sputtering," J. Vac. Sci. Technol.: B **37**, 021203 (2019).

[6] P. Polakowski and J. Müller, "Ferroelectricity in undoped hafnium oxide," Appl. Phys. Lett. **106**, 232905 (2015).

[7] F. Esaka, K. Furuya, H. Shimada, M. Imamura, N. Matsubayashi, H. Sato, A. Nishijima, A. Kawana, H. Ichimura, and T. Kikuchi, "Comparison of surface oxidation of titanium nitride and chromium nitride films studied by x-ray absorption and photoelectron spectroscopy," J. Vac. Sci. Technol., A **15**, 2521–2528 (1997).

[8] T. Shimizu, T. Yokouchi, T. Oikawa, T. Shiraishi, T. Kiguchi, A. Akama, T. J. Konno, A. Gruverman, and H. Funakubo, "Contribution of oxygen vacancies to the ferroelectric behavior of $Hf_{0.5}Zr_{0.5}O_2$ thin films," Appl. Phys. Lett. **106**, 112904 (2015).

[9] P. D. Lomenzo, Q. Takmeel, C. Zhou, C. M. Fancher, E. Lambers, N. G. Rudawski, J. L. Jones, S. Moghaddam, and T. Nishida, "TaN interface properties and electric field cycling effects on ferroelectric Si-doped HfO_2 thin films," J. Appl. Phys. **117**, 134105 (2015).

[10] B. Max, M. Pesic, S. Slesazeck, and T. Mikolajick, "Interplay between ferroelectric and resistive switching in doped crystalline HfO_2," J. Appl. Phys. **123**, 134102 (2018).

[11] D. Zhou, J. Xu, Q. Li, Y. Guan, F. Cao, X. Dong, J. Müller, T. Schenk, and U. Schröder, "Wake-up effects in Si-doped hafnium oxide ferroelectric thin films," Appl. Phys. Lett. **103**, 192904 (2013).

[12] M. H. Park, H. J. Kim, Y. J. Kim, Y. H. Lee, T. Moon, K. D. Kim, S. D. Hyun, F. Fengler, U. Schroeder, and C. S. Hwang, "Effect of Zr content on the wake-up effect in $Hf_{1-x}Zr_xO_2$ films," ACS Appl. Mater. Interfaces **8**, 15466–15475 (2016).

[13] U. Schroeder, C. Richter, M. H. Park, T. Schenk, M. Pešić, M. Hoffmann, F. P. G. Fengler, D. Pohl, B. Rellinghaus, C. Zhou, C.-C. Chung, J. L. Jones, and T. Mikolajick, "Lanthanum-doped hafnium oxide: A robust ferroelectric material," Inorg. Chem. **57**, 2752–2765 (2018).

[14] T. Shimizu, K. Katayama, and H. Funakubo, "Epitaxial growth of $YO_{1.5}$ doped HfO_2 films on (100) YSZ substrates with various concentrations," Ferroelectrics **512**, 105–110 (2017).

[15] H. J. Kim, M. H. Park, Y. J. Kim, Y. H. Lee, T. Moon, K. D. Kim, S. D. Hyun, and C. S. Hwang, "A study on the wake-up effect of ferroelectric $Hf_{0.5}Zr_{0.5}O_2$ films by pulse-switching measurement," Nanoscale **8**, 1383–1389 (2016).

[16] E. D. Grimley, T. Schenk, X. Sang, M. Pešić, U. Schroeder, T. Mikolajick, and J. M. LeBeau, "Structural changes underlying field-cycling phenomena in ferroelectric HfO_2 thin films," Adv. Electron. Mater. **2**, 1600173 (2016).

[17] M. Pešić, F. P. G. Fengler, L. Larcher, A. Padovani, T. Schenk, E. D. Grimley, X. Sang, J. M. LeBeau, S. Slesazeck, U. Schroeder, and T. Mikolajick, "Physical mechanisms behind the field-cycling behavior of HfO_2-based ferroelectric capacitors," Adv. Funct. Mater. **26**, 4601–4612 (2016).

[18] F. P. G. Fengler, M. Hoffmann, S. Slesazeck, T. Mikolajick, and U. Schroeder, "On the relationship between field cycling and imprint in ferroelectric," J. Appl. Phys. **123**, 204101 (2018).

[19] S. Starschich, S. Menzel, and U. Böttger, "Evidence for oxygen vacancies movement during wake-up in ferroelectric hafnium oxide," Appl. Phys. Lett. **108**, 032903 (2016).

[20] S. Starschich, S. Menzel, and U. Böttger, "Pulse wake-up and breakdown investigation of ferroelectric yttrium doped HfO_2," J. Appl. Phys. **121**, 154102 (2017).

[21] G. Walters, A. Shekhawat, N. G. Rudawski, S. Moghaddam, and T. Nishida, "Tiered deposition of sub-5nm ferroelectric $Hf_{1-x}Zr_xO_2$ films on metal and semiconductor substrates," Appl. Phys. Lett. **112**, 192901 (2018).

© Author(s) 2019